

Long-Term Crustal Deformation along the Southern Java Subduction Margin Revealed by GNSS Observations

Vira Friska^{1*}, Marzuki Marzuki², Nurdin Nurdin², Fadilla Monica²

¹Department of Physics, Universitas Riau, Pekanbaru 28293, Indonesia

²Department of Physics, Universitas Andalas, Padang, 25163, Indonesia

Article Info

Article History:

Received September 01, 2025
Revised January 28, 2026
Accepted February 14, 2026
Published online February 23, 2026

Keywords:

InaCORS data
Interseismic phase
Plate velocity
Southern Java
Subduction zone

Corresponding Author:

Vira Friska,
Email: vira.friska@lecturer.unri.ac.id

ABSTRACT

This study examines long-term GNSS-derived velocities along southern Java during 2011–2020 to characterize regional crustal deformation. Data from six InaCORS stations operated by BIG were processed using GAMIT/GLOBK to produce time series and estimate horizontal and vertical velocities. Horizontal velocities range from 21.35 mm/yr to 27.54 mm/yr toward the southeast, reflecting strong Eurasian Plate influence. The time series indicates gradual, continuous displacement without significant co-seismic offsets, despite several $M_w \sim 6$ earthquakes in the region. Vertical velocities show both uplift and subsidence, ranging from -13.84 mm/yr to 12.61 mm/yr, likely resulting from combined tectonic and non-tectonic processes. Because vertical GNSS measurements generally have higher uncertainty, these results must be interpreted cautiously. Although station motions appear stable, this does not indicate low seismic hazard. Instead, it may suggest ongoing strain accumulation within a seismic gap that could generate a future major earthquake. Overall, these findings enhance understanding of southern Java's subduction dynamics and support improved earthquake hazard assessment and disaster preparedness.

Copyright © 2026 Author(s)

1. INTRODUCTION

Java Island is one of the earthquake-prone regions in Indonesia due to the presence of several active tectonic mechanisms in this region. One of them is the Indo-Australian Plate subduction zone located to the south of Java Island, which is one of the most tectonically active plate boundaries in the world. (Bock et al., 2003; McCaffrey, 2009). This subduction zone extends from the Andaman Sea in northern Aceh to Sumbawa Island in the south (Grevemeyer & Tiwari, 2006; Jones et al., 2014; Schlüter et al., 2002). Although the frequency of seismic activity in southern Java is lower compared to Sumatra, the region remains within an active subduction zone and poses a significant risk of large earthquakes. Several major historical earthquakes have been recorded in the region, including the 1994 Banyuwangi earthquake (M_w 7.8) and the 2006 Pangandaran earthquake (M_w 7.7) (Mori et al., 2007; Xia et al., 2021), both of which triggered tsunamis and caused severe damage along the southern coast of Java. Additionally, the Java Sea earthquakes of 1921 and 1937 indicate that the seismic threat in this region should not be underestimated. Since the 2006 Pangandaran earthquake, no major interplate earthquakes have been recorded along the southern margin of Java. However, the absence of large seismic events does not necessarily indicate tectonic stability, as crustal deformation may continue without being expressed through major earthquakes. Therefore, the southern part of Java represents a critical area for

continuous geodetic monitoring to characterize ongoing deformation processes along the subduction margin.

In recent years, a number of moderate-magnitude earthquakes ($M_w > 5$) have also occurred in southern Java, with 22 events recorded in 2022, 17 events in 2023, 18 events in 2024 (including one earthquake with magnitude M_w 6.1), and 7 events in the first half of 2025 (USGS, 2025). Although most of these earthquakes were not major events, their occurrence confirms that the subduction zone off southern Java remains tectonically active and warrants continuous monitoring. This seismic threat is directly linked to the subduction of the Indo-Australian Plate beneath the Eurasian Plate. The plate convergence along the Java subduction zone is nearly orthogonal to the plate boundary, with a subduction rate of approximately 60–70 mm per year (Kopp et al., 2006). It differs from the Sumatra subduction zone, where plate convergence occurs at an oblique angle (Bradley et al., 2017). As a result of this subduction geometry, significant tectonic stress is associated with interplate interaction, contributing to the potential for large earthquakes along the southern Java subduction zone.

One effective approach for monitoring tectonic deformation is geodetic observation using the Global Navigation Satellite System (GNSS) (Arisa et al., 2021; Friska et al., 2022; Marzuki et al., 2022; Monica et al., 2022; Nurdin et al., 2023). This technology enables sub-millimeter accuracy in measuring plate displacement and allows for continuous monitoring of tectonic motion (Gunawan & Widiyantoro, 2019). In regions characterized by complex subduction systems, such as southern Java, long-term GNSS observations provide an effective way to document cumulative crustal deformation that may not always be expressed by frequent large earthquakes. Multiyear GNSS velocity also makes it possible to examine spatial variations in deformations, even during periods of relative seismic quiescence. In Indonesia, GNSS data from the Indonesia Continuously Operating Reference Station (InaCORS), operated by the Geospatial Information Agency (BIG), can be used for geodetic monitoring in tectonically active regions.

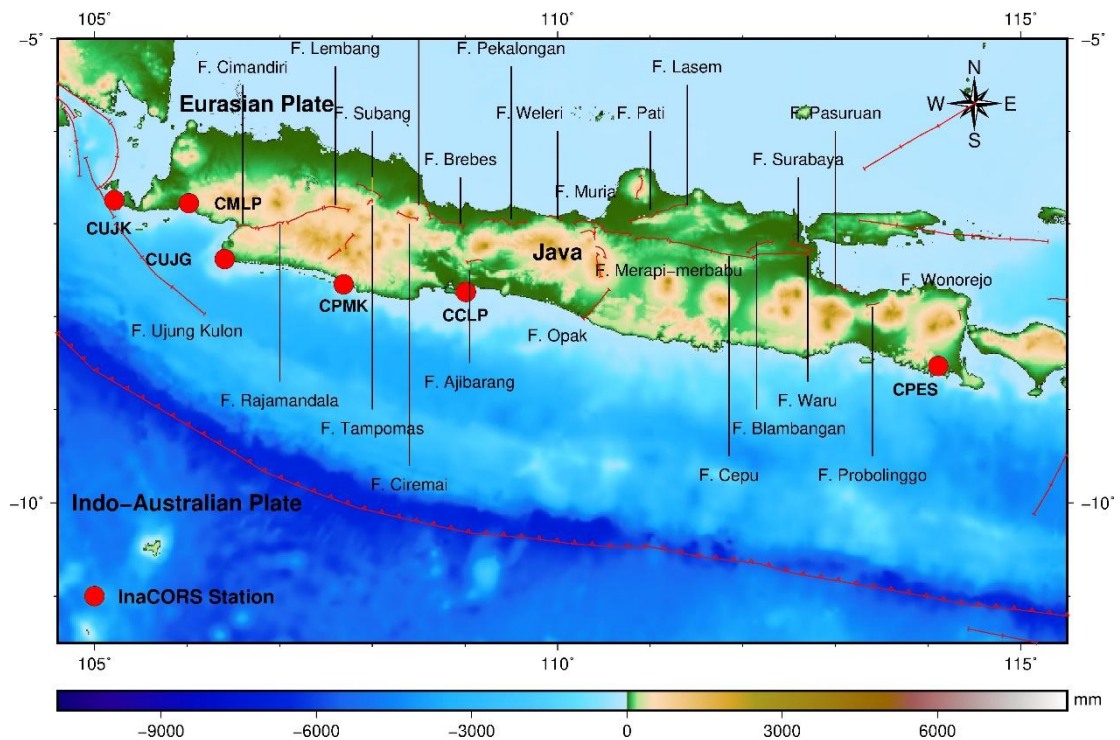


Figure 1 Geological map of Java showing major faults (abbreviated as F.) and the locations of InaCORS stations (red dots) used in this study. Plate boundaries are adapted from (Bird, 2003). Topography is based on the ETOPO1 Global Relief Model. Active faults in Java are from (PUSGEN, 2017).

Several previous geodetic studies have observed deformation in Java using GNSS observations. Hadi (2016) used GNSS data from InaCORS stations in southern Central Java (2013–2015) and showed

that all stations moved in a southeasterly direction at horizontal velocities ranging from 9 to 34 mm/year and vertical velocities ranging from -50 to +46 mm/year. Ramadian et al., (2018) reported consistent deformation rates of approximately 23.7 to 28.4 mm/year in Central Java from 2010 to 2016 based on GNSS observations in Central Java. Maulida et al., (2023) used continuous data from 2017 to 2022 and found horizontal velocities of up to 29 mm/year toward the southeast in East Java, as well as differences in patterns between the southern and northern regions of Java. Although these studies have provided valuable insights into crustal deformation across Java, systematic documentation of long-term GNSS-derived deformation patterns along the southern margin of Java remains limited.

To address this limitation, the present study analyzes long-term GNSS-derived velocity fields obtained from InaCORS stations distributed along the southern coast of Java during the period 2011–2020. The multi-year observation period enables the characterization of cumulative crustal deformation patterns in a tectonically active subduction environment, even in the absence of major interplate earthquakes during the study interval. By providing an updated and regionally focused description of GNSS-observed deformation along southern Java, this study contributes to a better understanding of ongoing tectonic processes and supports the importance of sustained geodetic monitoring for seismic hazard assessment and disaster mitigation efforts.

2. METHOD

2.1 Observation Data

The data used in this study were obtained from GNSS observations conducted by InaCORS (Indonesia Continuously Operating Reference Station), a network managed by the Geospatial Information Agency (BIG). A total of six InaCORS stations located along the southern part of Java Island were selected for this research. The observations consist of dual-frequency carrier phase and pseudorange measurements recorded continuously with a 30-second sampling interval. These stations were selected based on data availability and their location along the south coast of Java Island, representing the mainland forearc region of the Indo-Australian-Eurasian subduction system. As there are no islands located directly above the subduction interface south of Java that are suitable for GNSS installation. The observational data span the period from 2011 to 2020, and the location of the stations is shown in Table 1.

Table 1 Location of InaCORS stations used in this study. Station distribution can be seen in Figure 1.

Station	Location	Longitude (deg)	Latitude (deg)
CUJK	Cikaung, Sumur	105.2134	-6.7466
CMLP	Malingping Selatan	106.0191	-6.7782
CUJG	Gunung Batu, Ciracap	106.4056	-7.3820
CPMK	Santolo, Pameungpeuk	107.6905	-7.6548
CCLP	Cilacap Selatan	109.0102	-7.7371

In general, most stations have good data completeness. For example, stations CCLP and CMLP recorded an average of 349 and 358 daily observations per year, corresponding to approximately 94–98% data coverage. Other stations like CPES also showed relatively stable completeness (>300 days/year, ~92%), except in 2013 when coverage dropped. Although stations such as CUJG and CUJK experienced significant data shortages in the early years, data availability improved markedly in later years, especially after 2015. Station CPMK showed moderate fluctuations (~75%), but overall, the available data is representative enough for long-term analysis.

The InaCORS stations operate in real time with high temporal resolution at one-second intervals. Their positional accuracy reaches millimeter-level precision in both horizontal and vertical components. This high spatial and temporal resolution enables the observation of crustal deformation associated with tectonic processes. The InaCORS network is distributed across Indonesia and is publicly accessible, making it a valuable resource for ongoing research and geodetic monitoring. In addition to the InaCORS data, this study also utilized supplementary data, including observations from IGS (International GNSS Service) stations, which were collected from 27 reference stations, as shown in

Figure 2. IGS precise ephemeris data containing satellite orbit information, broadcast ephemeris data providing satellite and orbit parameters, and auxiliary data for atmospheric, tidal, and weather modeling were utilized to reduce noise and disturbances in the transmission signals received by satellites from GNSS stations.

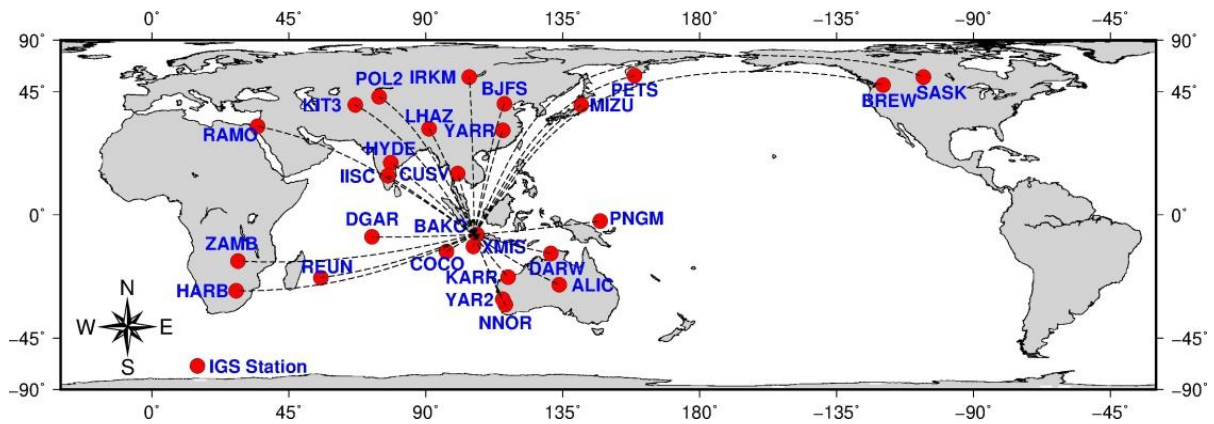


Figure 2 Locations of IGS stations. The dashed line indicates the IGS station used as a correction station.

2.2 Methodology

RINEX-formatted data (Receiver Independent Exchange Format) from observation stations were processed using the GAMIT/GLOBK software to obtain daily position data. The processing followed the methodology described by Herring et al. (2015), utilizing the Differential Global Positioning System (DGPS) technique, which requires fixed reference stations to improve positional accuracy. In this study, a set of reference stations from the International GNSS Service (IGS) network was integrated into the processing workflow. These stations were selected based on their optimal geographic distribution relative to the study area, ensuring better model convergence and precision.

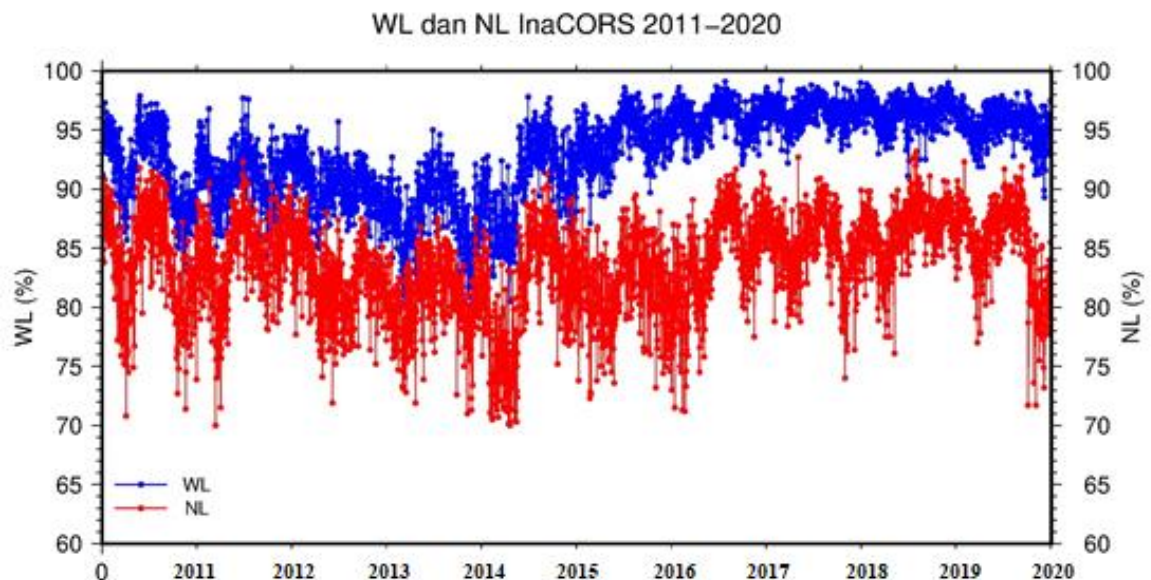


Figure 3 WL and NL values from the processing of InaCORS stations. Blue dots represent WL values, while red dots represent NL values.

The data processing using GAMIT produced several essential output files, including the h-file, which serves as input for the subsequent GLOBK processing, and the q-file, which contains analysis

results from the solve program, including data processing evaluations. One of the parameters found in this file is the fract value, which represents the ratio between the adjusted parameter estimate and its formal error. These parameter is used as an indicator to assess the quality of the GAMIT processing, where a fract value of less than 10 is considered acceptable for further processing with GLOBK (Herring et al., 2016). Another important file is the summary file, which provides information such as the number of stations, narrow lane (NL), wide lane (WL), and the postfit NRMS (normalized root mean square) value. The NL and WL parameters are used to evaluate potential errors or noise in the processing results. The standard threshold for NL > 70–80%, and for WL > 80–90% (Rwabudandi et al., 2019). The NL and WL values obtained from this study are presented in Figure 3, indicating that the data quality meets the required thresholds and is suitable for further processing.

The GLOBK software functions by integrating daily position data over an extended time period to estimate the average velocity of each station in both horizontal and vertical components. In this step, the GLOBK software integrates the daily position solutions obtained from GAMIT using a Kalman Filter. Through the least-squares fitting performed by the tsfit module, this approach estimates the most likely station position and velocity by minimizing the residuals between observed and modeled positions over time. Mathematically, the relationship between position $y(t)$ and time t can be expressed as (Tsai et al., 2015):

$$y(t) = a + bt_i + c \sin(2\pi t_i) + d \cos(2\pi t_i) + e \sin(4\pi t_i) + f \cos(4\pi t_i) + \sum_{j=1}^{n_g} g_j H(t - T_{gj}) + \sum_{j=1}^{n_h} h_j H(t_i - T_{hj}) + \sum_{j=1}^{n_k} k_j \exp\left[-\frac{t - T_{kj}}{\tau_j}\right] H(t - T) + \vartheta_i \quad (1)$$

Each daily solution epoch t_i (for $i = 1, \dots, N$) is given in years, and H is the Heavisine step function. The first two terms represent the site position (a) and its linear rate (b). Coefficients c and d describe the annual periodic motion, while e and f describe semi-annual motion. The next term corrects for any number n_g of offsets, with the magnitudes g and epochs T_g . The coefficients h and K_j are used for the post-seismic rate change and post-seismic exponential decay description with the relaxation time τ_j respectively. The final term ϑ_i , is the model residual.

GLOBK processing results are assessed using both log files and time series plots. The log files check the internal consistency of daily observations, while time series plots help detect unusual data points. The logs also provide statistical measures such as standard deviation, which support the analysis of the processed coordinates. Time series plots present weighted root mean square (WRMS) and normalized root mean square (NRMS) values. The WRMS values correspond to the north (V_n), east (V_e), and up (V_u) components. Typically, a WRMS value under 10 mm indicates reliable data without significant outliers (Herring et al., 2015). The resulting velocities were visualized using Generic Mapping Tools (GMT) 5.4.5 and further analyzed to examine spatial patterns of crustal deformation within the study area.

3. RESULTS AND DISCUSSION

3.1 Analysis of Time-Series Graph

Time series graphs for InaCORS stations along the south coast of Java are presented in Figure 4, divided into three: (a) east–west movement, (b) north–south movement, and (c) up–down movement. The x-axis represents the year of observation, while the y-axis indicates positional changes in each respective direction. The time series graphs do not show any clear or pronounced coseismic offsets at the observation stations during the study period. This absence of clear coseismic offsets could be attributed to the lack of major earthquakes on Java Island between 2011 and 2020, or the possibility of earthquakes, but their epicenters are far enough away from the observation stations that the jumps recorded in the time series are very small or even not clearly visible. Therefore, the observation period is suitable for examining long-term GNSS position variations and evaluating the overall stability of the time series used for velocity estimation.

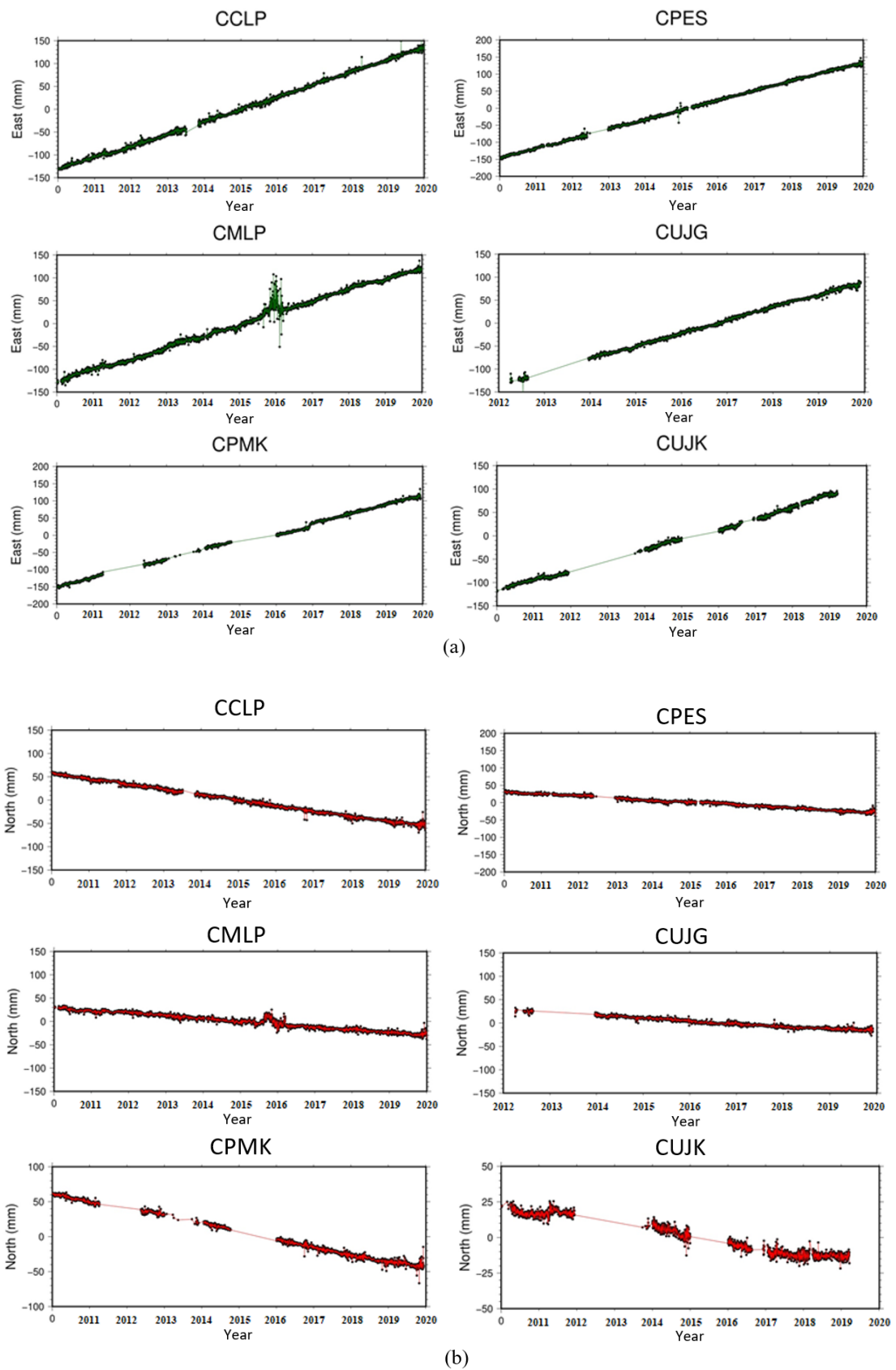


Figure 4 Time series graph (a) eastward component (b) northward component.

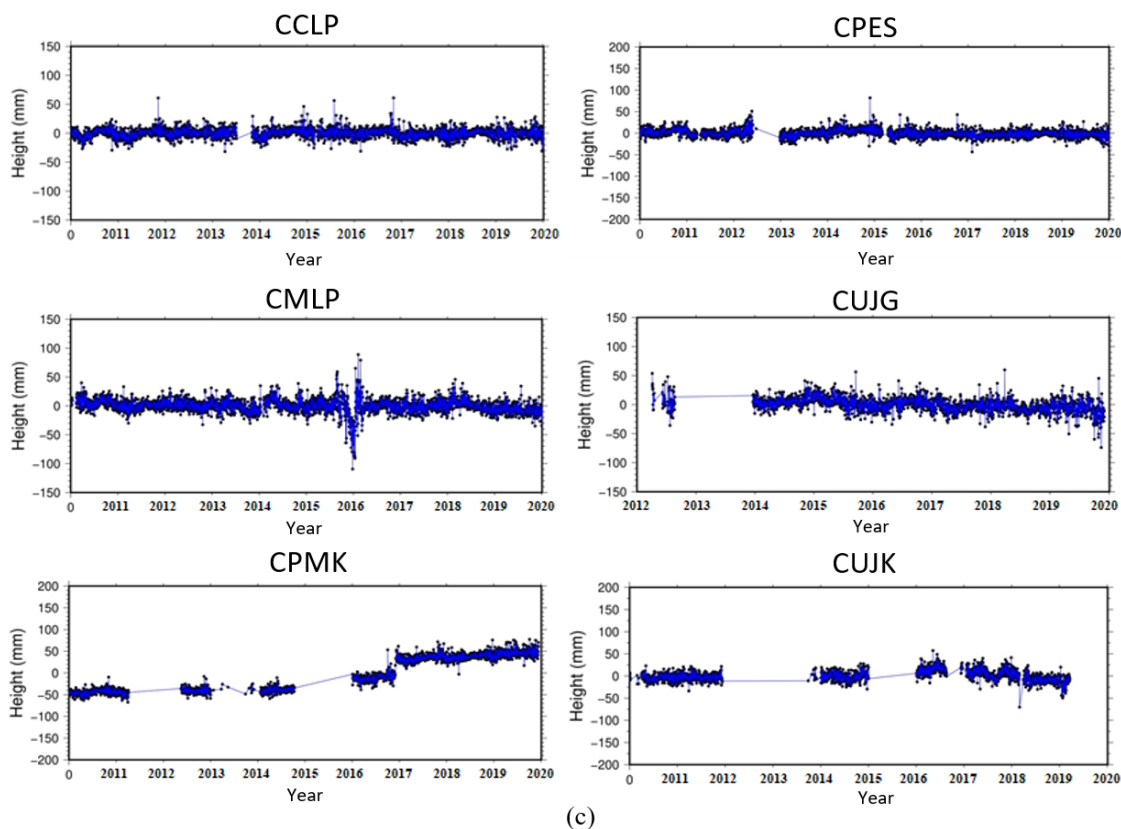


Figure 4 (continued) (c) vertical component.

According to data from the USGS, only eight earthquakes with magnitudes greater than 6 occurred in the southern region of Java and its subduction zone between 2011 and 2020. These seismic events include the Mw 6.7 earthquake on April 4, 2011 (off the southern coast of West Java); the Mw 6.1 event on October 13, 2011 (southern coast of East Java/Bali region); the Mw 6.1 earthquake on September 3, 2012 (southern Central–East Java); the Mw 6.7 event on June 13, 2013 (south of Central Java); the Mw 6.1 quake on January 25, 2014 (southern Central Java); the Mw 6.1 event on April 6, 2016 (southern Java region); the Mw 6.5 earthquake on December 15, 2017 (off southern West Java); and the Mw 6.9 event on August 2, 2019 (southern West Java/Sunda Strait region). Among these, three earthquakes had epicenters around the subduction zone, while the rest occurred closer to the mainland of Java but still in the southern region of Java. For example, the magnitude 6.9 earthquake on August 2, 2019 (USGS, 2025) occurred at a distance of 75.6 km from the CUJK station, but no co-seismic spikes were observed in the station's time series. The lack of clear coseismic offsets in the time series suggests that no major instantaneous displacements were recorded at the GNSS stations during the study period, allowing the analysis to focus on longer-term deformation trends rather than abrupt seismic-related offsets.

From the time series graphs (based on the east-west and north-south direction), it can be seen that the horizontal movement of the station tends to be consistent with the pattern of movement towards the southeast. However, there are data gaps at certain times, which may be caused by technical disturbances, such as GNSS satellite signal interference due to heavy rainfall, which affects signal quality and data accuracy. Most stations have high data coverage (≥ 300 days/year), which supports the robustness of the estimated long-term velocities. Stations such as CCLP and CMLP consistently record observations for the full year, resulting in strong linear trends. In contrast, CUJG and CUJK experienced a critical lack of data in the early years, resulting in the exclusion of those years from the velocity estimates. In addition, routine maintenance or hardware failures can also be a contributing factor to data

gaps. At the end of 2016, the CMLP station's time series graph showed unusual fluctuations. Based on the evaluation of data processing, the parameters used as quality indicators in the GAMIT analysis for 2016 met the required standards (see Methodology section). The observed fluctuations are likely associated with data quality issues during that period, such as cycle slips, multipath effects, or temporary receiver and antenna disturbances. (Blewitt & Lavallée, 2002; Williams et al., 2004). This interpretation is further supported by the absence of significant seismic activity around the CMLP station during that year.

3.2 Horizontal and Vertical Plate Motion

The time series graphs of stations in southern Java show no clear or pronounced coseismic offsets during the 2011-2020 observation period (Figure 4), allowing the estimation of long-term GNSS-derived velocities based on linear trends in the multi-year time series. The estimated horizontal and vertical velocity components are summarized in Table 2, while the overall movement directions of the stations are illustrated in Figure 5. Based on the velocity calculations, the horizontal velocities of all observation stations during the 2011-2020 period show the same movement direction, namely toward the southeast. This similarity in movement direction reflects the uniformity of regional deformation patterns along the southern coast of Java. It also indicates that these stations are responding to large-scale deformation processes occurring along the southern margin of Java. The consistency of this movement direction also supports the reliability of velocity estimates obtained from multi-year GNSS time series.

Table 2 Station velocities and movement directions during 2011-2020. V_e and V_n , represent the eastward and northward velocity components, respectively

Station	V_e (mm/yr)	V_n (mm/yr)	Horizontal velocity (mm/yr)	Direction (°)	Vertical velocity (mm/yr)
CUJK	21.26	-1.92	21.35	S16.28E	12.61
CMLP	21.66	-7.19	22.82	S18.36E	-2.72
CUJG	27.35	-3.19	27.53	S13.46E	-13.84
CPMK	23.50	-8.80	25.09	S20.53E	1.96
CCLP	26.02	-7.60	27.11	S6.65E	2.70
CPES	23.53	-5.63	24.19	S5.16E	-2.22

The horizontal velocity obtained from processing InaCORS station data during the 2011-2020 period ranged from 21.35 to 27.54 mm/yr. This horizontal velocity shows systematic spatial variation from west to east. Stations located in the southwestern part of Java, such as CUJK and CMLP, show relatively smaller horizontal velocities of ~21-23 mm/yr, with CUJK recording the smallest velocity among all stations. Conversely, the CUJG, CCLP, and CPMK stations located in the central southern segment of Java show higher horizontal velocities of ~25-27 mm/yr, with the highest value observed at CUJG (27.54 mm/yr). These velocities are comparable to the results reported by Ramadian et al., 2018, who estimated the horizontal velocity of GPS stations in Central Java during the period 2010-2015 to be 23.7-28.4 mm/year. Although the observation periods and station configurations differ, the similarity in the value ranges suggests consistent long-term deformation patterns in Central Java and surrounding areas.

Meanwhile, the station located in the southeastern part of Java, CPES, exhibits an intermediate horizontal velocity of 24.19 mm/yr. This value is comparable to the results reported by Rwabudandi et al. (2019), who recorded an average velocity of approximately 26.38 mm/year with a southeastward movement for GNSS stations in East Java during the period 2015-2018. On the other hand, Maulida et al. (2023) reported a slightly higher southeasterly velocity of around 29 mm/year for the period 2017-2022. These differences suggest slight temporal variations between observation periods, without changing the general pattern of regional movement in East Java. From the east-west and north-south velocity components, the resulting motion is also coherent, with positive east-west and negative north-south components, producing a southeastward movement direction.

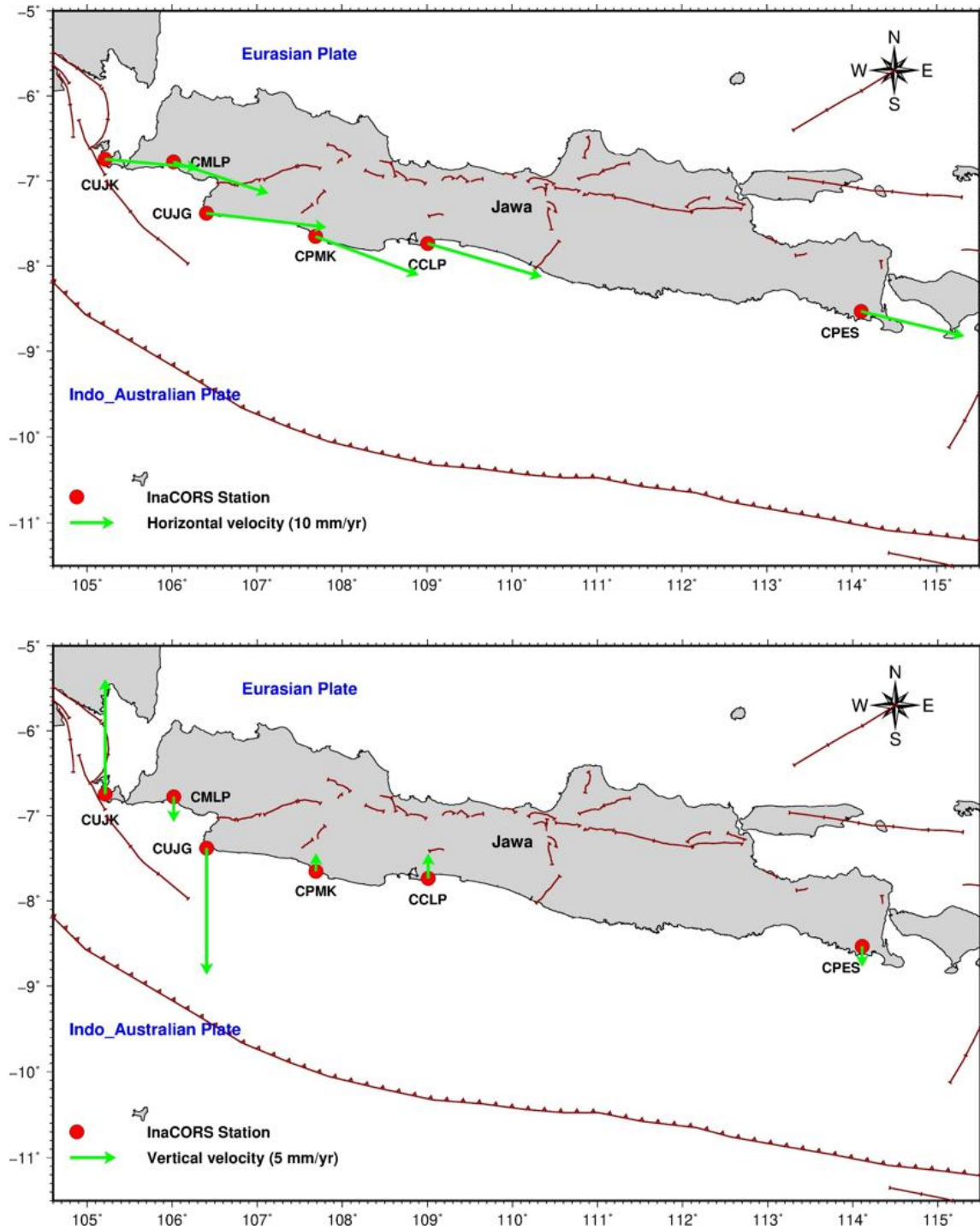


Figure 5 GNSS-derived velocities along southern Java: (a) horizontal and (b) vertical components. Each arrow represents the average station velocity estimated from GLOBK solutions for the corresponding year.

When viewed along the west-east transect of southern Java (Table 2), the horizontal movement directions do not show a systematic pattern comparable to the velocity magnitudes. However, all observation stations show a consistent movement towards the southeast, with a relatively small angle range, namely around S5°E to S20°E. This relatively small range of directions suggests a coherent regional deformation pattern along the southern coast of Java. In GNSS velocity analysis, relatively small angle differences between stations are reasonable because movement direction is strongly

influenced by the ratio between the east and north velocity components. Small changes in one of the components, especially the north-south component, will result in angle variations of several degrees without changing the general character of regional movement. Therefore, the observed angle variations reflect local spatial variations and do not necessarily indicate differences in tectonic processes.

Small variations in station movement directions may be influenced by the relative position of the stations with respect to the forearc region, the orientation of the coastline, and local tectonic conditions along southern Java. These factors can lead to differences in the orientation of velocity vectors between stations without changing the dominant direction of motion, which remains southeastward. Therefore, although the movement directions do not show a uniform pattern in the same way as the velocity magnitudes, the similarity in the overall direction indicates that GNSS motion in southern Java is influenced by regional-scale tectonic processes.

In contrast to the horizontal component, the vertical velocities of the observation stations show relatively large variations. Several stations exhibit an uplift tendency, as observed at station CUJK with a value of 12.61 mm/yr, which represents the largest uplift among the analyzed stations. Geomorphologically, the island of Java sits on top of the Eurasian Plate, which is being thrust by the subducting Indo-Australian Plate, so a tendency toward uplift is natural (Verstappen, 2010). In contrast, other stations show subsidence or near-zero values, with station CUJG recording the largest downward motion (indicated by a negative value) of 13.84 mm/yr, which may be more influenced by anthropogenic factors such as excessive groundwater extraction (Chaussard et al., 2013). Unlike the relatively uniform direction of horizontal motion, vertical motion patterns provide a more dynamic picture along southern Java. This observation suggests that vertical motion is more strongly influenced by a combination of tectonic processes and local factors. Therefore, further in-depth analysis is required to better understand the impact of external factors on the dynamics of these stations and to strengthen the interpretation of tectonic processes in the southern coastal region of Java.

It should be emphasized that the station velocities presented in this study represent total velocities over the 2011-2020 period, calculated using the velocity estimation module in GLOBK. These velocities may include contributions from various deformation processes, including long-term tectonic deformation as well as residual postseismic effects that may still persist from earlier earthquakes, such as the 2006 Pangandaran earthquake. The analysis in this study is focused on describing the spatial patterns of GNSS-derived velocities observed during the observation period. This approach is consistent with the objective of the study, which is to document the general characteristics of crustal motion along southern Java based on the available GNSS data.

Overall, the long-term GNSS velocity field along southern Java provides a regional view of cumulative crustal deformation over the past decade. The consistent southeastward horizontal motion, together with the systematic spatial variation in velocity magnitudes, indicates that crustal deformation along the southern Java margin is controlled by regional-scale tectonic processes. This movement pattern is consistent with the motion of the Eurasian Plate (Bock et al., 2003; Simons et al., 2007), reflecting the dominant influence of plate motion on the observation stations located on the Eurasian Plate. Accordingly, the results of this study provide an important long-term GNSS velocity reference that can serve as a baseline for sustained geodetic monitoring and as a foundation for future deformation studies and seismic hazard assessment in southern Java.

4. CONCLUSION

This study documents long-term horizontal GNSS-derived velocities at six observation stations along the southern coast of Java, showing the dominant influence of the Eurasian Plate movement with average horizontal velocity values of 21.35 to 27.54 mm/yr. Although non-tectonic processes may contribute to the observed velocities (Blewitt & Lavallée, 2002), the overall coherence of the motion indicates that the estimates primarily reflect long-term crustal deformation over the observation period. Variations in vertical velocities were also observed, reflecting the more complex nature of vertical deformation that may involve both tectonic and non-tectonic processes. The deformation patterns observed up to 2020 indicate that crustal deformation along the southern Java margin remains active

and spatially coherent, as reflected by the long-term GNSS-derived velocity. These findings highlight the importance of sustained geodetic monitoring to improve understanding of long-term crustal deformation processes in this tectonically active region. In addition, this study provides a useful observational baseline for future research aimed at further investigating long-term deformation processes along the southern Java subduction margin. Future studies would benefit from longer observation periods, particularly where multi-decade GNSS data are available, as well as increased GNSS station density along the southern coast of Java to enhance spatial resolution and reduce uncertainty in deformation estimates. In addition, future analyses may further refine the interpretation of GNSS-derived velocities by explicitly accounting for postseismic deformation processes, especially in regions influenced by large historical earthquakes.

ACKNOWLEDGEMENT,

The present study was supported by the 2021 Research Grants for Publication to Support the Professor Acceleration Program from Universitas Andalas (PDU-KRP2GB-UNAND) (contract no: T/11/UN.16.17/PP.IS-PDU-KRP2GB-Unand/LPPM/2021). The authors would also like to express their sincere gratitude to Dr. Deasy Arisa from the National Research and Innovation Agency (BRIN), Indonesia, for her valuable guidance throughout this research. Furthermore, we thank the Geospatial Information Agency (BIG) of Indonesia for providing access to the InaCORS (Indonesia Continuously Operating Reference Station) data used in this study.

REFERENCE,

- Arisa, D., Setiadi, B., & Priyanto, W. S. (2021). Pre-and Coseismic Analysis of the Mw7.6 Padang Earthquake 2009 from Geodetic Approach. *IOP Conference Series: Earth and Environmental Science*, 789(1), 012069. <https://doi.org/10.1088/1755-1315/789/1/012069>
- Bird, P. (2003). An updated digital model of plate boundaries. *Geochemistry, Geophysics, Geosystems*, 4(3). <https://doi.org/10.1029/2001GC000252>
- Blewitt, G., & Lavallée, D. (2002). Effect of annual signals on geodetic velocity. *Journal of Geophysical Research: Solid Earth*, 107(B7), ETG-9.
- Bock, Y., Prawirodirdjo, L., Genrich, J. F., Stevens, C. W., McCaffrey, R., Subarya, C., Puntodewo, S. S. O., & Calais, E. (2003). Crustal motion in Indonesia from global positioning system measurements. *Journal of Geophysical Research: Solid Earth*, 108(B8).
- Bradley, K. E., Feng, L., Hill, E. M., Natawidjaja, D. H., & Sieh, K. (2017). Implications of the diffuse deformation of the Indian Ocean lithosphere for slip partitioning of oblique plate convergence in Sumatra. *Journal of Geophysical Research: Solid Earth*, 122(1), 572–591.
- Chaussard, E., Amelung, F., Abidin, H., & Hong, S.-H. (2013). Sinking cities in Indonesia: ALOS PALSAR detects rapid subsidence due to groundwater and gas extraction. *Remote Sensing of Environment*, 128, 150–161.
- Friska, V., Arisa, D., Marzuki, M., & Monica, F. (2022). Indo-Australian Plate Velocity Measurement During Interseismic Phase in 2010–2014 Using Sumatran GPS Array (SuGAR) Data. *Proceedings of the International Conference on Radioscience, Equatorial Atmospheric Science and Environment and Humanosphere Science, 2021*, 925–934.
- Grevemeyer, I., & Tiwari, V. M. (2006). Overriding plate controls spatial distribution of megathrust earthquakes in the Sunda–Andaman subduction zone. *Earth and Planetary Science Letters*, 251(3–4), 199–208.
- Gunawan, E., & Widiyantoro, S. (2019). Active tectonic deformation in Java, Indonesia inferred from a GPS-derived strain rate. *Journal of Geodynamics*, 123, 49–54.
- Hadi, A. L. (2016). Analisa Deformasi Di Wilayah Jawa Tengah Bagian Selatan Menggunakan GPS-CORS Tahun 2013-2015. *Jurnal Teknik ITS*, 5(2), C70-C74. <https://doi.org/10.12962/j23373539.v5i2.17209>
- Herring, T. A., King, R. W., Floyd, M. A., & McClusky, S. C. (2015). *GLOBK Reference Manual. Global Kalman filter VLBI and GPS analysis program Release 10.6. June*, 1–95.
- Herring, T. A., Melbourne, T. I., Murray, M. H., Floyd, M. A., Szeliga, W. M., King, R. W., Phillips, D. A., Puskas, C. M., Santillan, M., & Wang, L. (2016). Plate Boundary Observatory and related networks: GPS data analysis methods and geodetic products. *Reviews of Geophysics*, 54(4), 759–808.

- Jones, E. S., Hayes, G. P., Bernardino, M., Dannemann, F. K., Furlong, K. P., Benz, H. M., & Villaseñor, A. (2014). *Seismicity of the Earth 1900-2012 Java and vicinity*. US Geological Survey.
- Kopp, H., Flueh, E. R., Petersen, C. J., Weinrebe, W., Wittwer, A., & Scientists, M. (2006). The Java margin revisited: Evidence for subduction erosion off Java. *Earth and Planetary Science Letters*, 242(1–2), 130–142.
- Marzuki, Ramadhan, R., Friska, V., Primadona, H., Ramadhan, R. A., Monica, F., Arisa, D., & Namigo, E. L. (2022). Dynamics of West Coast of Sumatra and Island Arc Mentawai during the Coseismic Phase of the Mentawai Mw7.8 25 October 2010 Earthquake. *Journal of Physics: Conference Series*, 2309(1), 012030. <https://doi.org/10.1088/1742-6596/2309/1/012030>
- Maulida, P., Rafiq, M., Herawati, Y. A., Kurniawan, A., & Taufik, M. (2023). Current deformation in eastern part of Java derived from GPS observation 2017-2022. *IOP Conference Series: Earth and Environmental Science*, 1276(1), 12023.
- McCaffrey, R. (2009). The tectonic framework of the Sumatran subduction zone. *Annual Review of Earth and Planetary Sciences*, 37(1), 345–366.
- Monica, F., Friska, V., Arisa, D., & Marzuki, M. (2022). Comparison of Deformation Vectors Due to Earthquake in Subduction Zone and Sumatran Fault for Each Phase of Earthquake Cycle. *Jurnal Ilmu Fisika | Universitas Andalas*, 14(2), 73–85. <https://doi.org/10.25077/jif.14.2.73-85.2022>
- Mori, J., Mooney, W. D., Afnimar, Kurniawan, S., Anaya, A. I., & Widiyantoro, S. (2007). The 17 July 2006 tsunami earthquake in west Java, Indonesia. *Seismological Research Letters*, 78(2), 201–207.
- Nuridin, N., Pujiastuti, D., & Marzuki, M. (2023). Analysis of vertical seismic deformation of the 2018 Palu earthquake using Global Navigation Satellite System (GNSS) data. *Journal of Physics: Conference Series*, 2596(1), 12037.
- PUSGEN. (2017). *Peta Sumber Dan Bahaya Gempa Indonesia Tahun 2017*. Pusat Penelitian dan Pengembangan Perumahan dan Permukiman. <https://simantu.pu.go.id/content/?id=3605>
- Ramadian, R. R., Meilano, I., Hanifa, N. R., & Efendi, J. (2018). Interseismic coupling off the south of Central Java from GPS-derived baseline change rates. *AIP Conference Proceedings*, 1987(1), 20105.
- Rwabudandi, I., Anjasmar, I. M., & Susilo, S. (2019). Evaluating GPS CORS Data for Crustal Deformation Analysis in East Java. *Jurnal Teknik ITS*, 8(2). <https://doi.org/10.12962/j23373539.v8i2.49686>
- Schlüter, H. U., Gaedicke, C. H., Roeser, H. A., Schreckenberger, B., Meyer, H., Reichert, C. H., Djajadihardja, Y., & Prexl, A. (2002). Tectonic features of the southern Sumatra-western Java forearc of Indonesia. *Tectonics*, 21(5), 11.
- Simons, W. J. F., Socquet, A., Vigny, C., Ambrosius, B. A. C., Haji Abu, S., Promthong, C., Subarya, C., Sarsito, D. A., Matheussen, S., & Morgan, P. (2007). A decade of GPS in Southeast Asia: Resolving Sundaland motion and boundaries. *Journal of Geophysical Research: Solid Earth*, 112(B6).
- Tsai, M. C., Yu, S. B., Shin, T. C., Kuo, K. W., Leu, P. L., Chang, C. H., & Ho, M. Y. (2015). Velocity field derived from Taiwan continuous GPS Array (2007-2013). *Terrestrial, Atmospheric and Oceanic Sciences*, 26(5), 527–556. [https://doi.org/10.3319/TAO.2015.05.21.01\(T\)](https://doi.org/10.3319/TAO.2015.05.21.01(T))
- USGS. (2025). *USGS Earthquake Catalog Search*. <https://earthquake.usgs.gov/earthquakes/search/>
- Verstappen, H. T. (2010). Indonesian landforms and plate tectonics. *Indonesian Journal on Geoscience*, 5(3), 197–207.
- Williams, S. D. P., Bock, Y., Fang, P., Jamason, P., Nikolaidis, R. M., Prawirodirdjo, L., Miller, M., & Johnson, D. J. (2004). Error analysis of continuous GPS position time series. *Journal of Geophysical Research: Solid Earth*, 109(B3).
- Xia, Y., Geersen, J., Klaeschen, D., Ma, B., Lange, D., Riedel, M., Schnabel, M., & Kopp, H. (2021). Marine forearc structure of eastern Java and its role in the 1994 Java tsunami earthquake. *Solid Earth Discussions*, 2021, 1–19.